Face Recognition in 2D and 2.5D using Ridgelets and Photometric Stereo

Satyajit N. Kautkar, Gary A. Atkinson, Melvyn L. Smith

Machine Vision Laboratory, University of the West of England, Bristol, BS16 1QY, UK

Abstract

A new technique for face recognition – *Ridgefaces* – is presented. The method combines the well-known Fisherface method with the ridgelet transform and high-speed Photometric Stereo (PS). The paper first derives ridgelet projections for 2D/2.5D face images before the Fisherface approach is used to reduce the dimensionality and increase the spread of the resulting feature vectors. The ridgelet transform is attractive because it is efficient at extracting highly discriminating low-frequency directional features. Best recognition is obtained when Ridgefaces is performed on surface normals acquired from PS, although good results are also found using standard 2D images and PS-derived albedo maps.

Keywords: Face recognition, ridgelet transform, photometric stereo, dimensionality reduction

1. Introduction

Automatic face recognition is one of the most promising and potentially widespread areas of computer vision. It has attracted a large amount of research interest due to its non-intrusive nature compared to other biometrics. Indeed, machines now consistently outperform humans in many face recognition experiments [1]. However, despite great improvement in recognition accuracy

Email addresses: skautkar@gmail.com (Satyajit N. Kautkar), Gary.Atkinson@uwe.ac.uk (Gary A. Atkinson), Melvyn.Smith@uwe.ac.uk (Melvyn L. Smith)

for contrived set-ups over recent years, a method that is robust to pose and illumination changes and is efficient in processing time and memory remains a major challenge.

In this paper, we make a significant contribution to automatic facial recognition technology by proposing a novel face recognition method which is applicable to both 2D and 2.5D/3D face data. We call this method "Ridgefaces". The method uses a combination of the ridgelet transform [2] and the widely known method of Fisherfaces [3] (using standard implementations of Principle Components Analysis (PCA) and Linear Discriminant Analysis (LDA)). The motivation for the use of ridgelets is that they achieve high levels of dimensionality reduction while maintaining highly discriminating directional information and low-frequency data but suppressing the less useful high-frequency features. While conventional data reduction methods, including PCA and LDA, are *statistically* optimised for generic data processing, we show that ridgelets are ideal for faces specifically, for the above reasons. Combining the methods gives the best overall data representation.

Our novel method can be summarised as follows. Firstly, albedo and surface normal data are acquired using Photometric Stereo (PS) [4]. We then apply the ridgelet transform to each image before the Fisherface algorithm is applied to the transformed images to further compress the data and maximise the distance between classes in the new subspace (and minimise the intra-class distance). Finally, the simple Euclidean distance between test and training images is used for classification.

The hardware set-up for construction of the testing database (called the "PhotoFace" database) is described in [5] and [6]. In summary, the device constructs face models using PS hardware and algorithms [5, 4] in which facial images are captured from the same viewpoint under different illumination directions. The albedo and surface normals are then estimated from the raw images and we experiment with Ridgefaces on both these modalities.

Aside from the novel methodology, the other principal contributions and advantages of the research are as follows:

- Our main testing dataset – the PhotoFace database – consists of face images captured as participants enter a busy workplace. Their presence is automatically detected by a sensor and the device is automatically triggered. This ensures that the data consists of a range of natural poses and expressions [5, 6].

- We applied our method to a range of databases including the above PhotoFace and several older 2D databases. This proves that our technique is robust to a range of "everyday" poses, illumination conditions and expressions, not just fully frontal faces with neutral expression.

- The paper reports a detailed set of experiments to investigate the performance variation with different algorithm parameters (e.g. coarseness of the discrete approximation to transforms, number of principal components used, etc.). Indeed, one of the key contributions of the paper is the optimisation of capture and processing methods and parameters.

- We prove that the nature of our ridgelet-based image representation is able to maintain a near-constant degree of discriminatory information, regardless of the coarseness of the approximation to the transforms and is highly robust to image resolution.

- We show that our method is highly competitive to the state-of-the-art in terms of recognition rate, processing time and storage requirements.

The remainder of the paper is organised as follows. Section 2 summarises the related work in 2D and 3D face recognition techniques and algorithms, in addition to relevant 3D reconstruction and representation methods. The background theory for our novel method is then described in Section 3. Section 4 provides the new methodology of the proposed algorithm. Detailed experimental results followed by a discussion are presented in Sections 5 and 6 respectively, before our findings are summarised in Section 7.

2. Related Work

The development of automatic face recognition systems started in the early 1960s when Bledsoe developed a system based on the geometrical information of face parts [7]. Since then, a variety of algorithms based on PCA and LDA have been developed, modified and tested consistently over the years. Turk and Pentland developed a face recognition method called *eigenfaces* based on PCA [8]. Kirby and Sirovich developed a PCA-based technique in which face images can be efficiently represented using eigenspace. In this method, accurate face representations can be modelled using a relatively small number of eigenvectors, reducing storage and processing time considerably, whilst maintaining high recognition rates [9].

One drawback of the eigenface method, is that while maximizing variances along given principle components, it retains unwanted variation due to the lightning, facial expressions and other factors. Later, the *Fisherface* method was devised [3], which is an extension of the LDA method developed by Fisher for class discrimination [10]. This method used Fisher discriminants to classify different feature vectors and produced well-separated classes in low dimensional subspace, giving better performance in varying lightning conditions and facial expressions. Unfortunately, LDA suffers from the small sample problem and so is less effective if only a small training set is available [11, 12].

Much more recently, Jadhav and Holambe used a face recognition technique based on Radon and wavelet transforms [13]. In this technique, directional features of the facial images are calculated in different orientations using the Radon transform which enhances low frequency components in that image. Then, a wavelet transform is applied in Radon space which produces a multi-resolution facial image. The ridgelet transform is the result of this 1D wavelet transform in the Radon domain. Ridgelet transforms are suitable for describing signals with high-dimensional singularities such as image lines. The Finite RIdgelet Transform (FRIT) is the discrete form of the continuous ridgelet transform [2]. Jun et al. proposed a new algorithm which digitally implements ridgelet trans-

forms suitable for images of dyadic length [14]. This method not only retains all the properties of the traditional FRIT but also extends the application of FRIT in image processing by improving the sensitivity to direction and increasing the angular resolution. The advantages of these Radon/ridgelet-based methods have partly motivated this paper, one of whose aims is to extend the methods to more general settings and 3D data.

While all the above research has shown promise with 2D images of faces, a large amount of current research into face recognition is based on the 3D information of facial geometry [15]. The motivation for most of this 3D work is that such geometric information can minimize the detrimental impact of changing illumination conditions and viewing angles, while also providing an overall richer dataset. The amount of research in the area is vast, so we concentrate on the most closely related contributions for this review.

An obvious hurdle for 3D methods is the initial need to acquire the 3D structure of each face – ideally from one or more 2D images. Early attempts to recover the 3D information of objects were made in 1970s; for example when Horn invented a technique to recover the shape of an object from its shading information [16]. A variety of techniques have been developed since then to estimate the shape of objects using various cues such as occluding boundaries [17] or texture [18].

One reconstruction technique that has proven practical for face recognition is PS [4, 19]. In this method, an object (or face) is imaged several times using a fixed 2D camera. Each image must be captured using a different light source direction. Hansen et al. have devised a near-real time PS system for 3D face capture that is easily deployable for many face recognition applications [5]. Zafeiriou et al. subsequently used this method to acquire a novel 3D face database with subjects captured under "natural" conditions [6]. A host of variations to PS for both general usage and faces specifically have also been suggested in the literature [20, 21, 22, 23, 24, 25, 26].

Blanz and Vetter developed a form of analysis-by-synthesis method for face shape estimation using a statistical model of human faces captured using a laser

scanner [27]. Smith and Hancock also use a statistical model, this time based on surface normals acquired using shape-from-shading [28]. Reiter et al. developed a method based on Canonical Correlation Analysis (CCA) which reconstructs 3D faces from RGB colour images [29]. They predicted the 3D depth map of faces using the CCA approach by relating the depth information of a face image with the appearance of the face. They modelled the combined effect of illumination direction, albedo and shape with correlated linear features in the space of depth images and colour images. Kim et al. developed a non-intrusive 3D face data acquisition system which uses an infrared line sensor pattern [30].

Mayo and Zhang developed a face recognition system which uses a 3D point cloud for recognition. They rotated the face points about the x, y and z axes and projected them iteratively onto a 2.5D image, thus extracting a small set of points for recognition [31]. Another method which uses local shape variation information is proposed by Xu et al. [32]. They also represent faces as 3D point clouds and construct feature vectors by combining the global geometric features and the local shape variation information.

Abate et al. developed a simple, fast and accurate recognition method in which a difference map is calculated from the comparison of normal maps of two faces [33]. The surface normals and curvature are represented by a polygonal mesh and then projected as an RGB image which is a 2D representation of a 3D mesh. Therefore, 3D recognition is effectively posed as a more efficient 2D recognition problem. Lu et al. developed a system in which both shape and texture information from a 2.5D scan are used [34]. The shapes of the two faces are matched using a modified Iterative Closest Point (ICP) algorithm [35]. From this, they select a set of closely matched candidates and apply LDA which reduces the complexity of the classification. A related approach by Papatheodorou and Rueckert can be seen in [36].

It is not always the case that 3D recognition will outperform 2D face recognition [37]. Consequently, in order to preserve the advantages of these two complementary modalities, Xue and Ding developed a multi-model boosting algorithm in which 3D range information is integrated with 2D image data [38].

This algorithm can detect features including faces, noses, eyes etc., which can then be used for recognition. Similar fusion of depth and texture information is used and compared by BenAbdelkader and Griffin [39]. Depth and texture maps are used separately and together for identification and verification. The best recognition rate of 100% for their particular dataset is achieved when the the information is combined. Kusuma and Chua implemented PCA based 2D+3D multimodal face recognition method which uses texture and shape information [40]. Both 2D and 3D images are recombined by projecting them into PCA subspace and then into fisherfaces to maximise the scatter. Related approaches can be found in [41, 42, 43, 44, 37, 45, 46].

Further reviews on 3D face recognition techniques in general are presented in [47, 48, 15, 49].

3. Background Theory

This section summarizes the main concepts and background theory used in the proposed method. This includes ridgelet transforms, subspace methods and PS.

3.1. Theory of Ridgelet Transforms

In many image processing tasks, a sparse representation of an image is used in order to compact the data into a relatively small number of samples while maintaining discriminating information. Wavelets are a good example of sparse geometrical image representation. But despite the success of wavelets, they exhibit efficiency limitations when applied in more than one dimension. In particular, wavelets fail to efficiently represent objects with highly anisotropic 2D elements such as lines or curvilinear structures (e.g. intensity edges). The reason is that wavelets are non-geometrical and do not exploit the regularity of the edge curve. Wavelets are therefore good at representing zero-dimensional or point singularities. However, two-dimensional piecewise smooth signals (such as face images) have one-dimensional singularities meaning that wavelets will not accurately represent the smoothness of the image along the curve [50, 2].

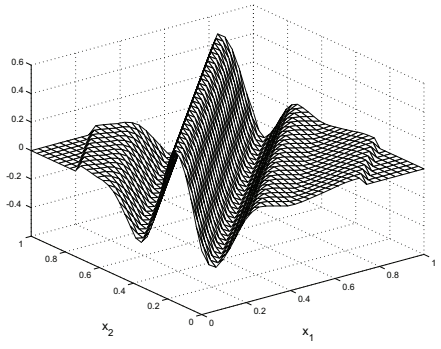

Figure 1: An example ridgelet function [50].

Motivated by the above limitations, Candies and Donoho recently developed ridgelets to deal with line singularities of the image in 2D [50]. The idea is to map a line singularity into a point singularity using the Radon transform. A wavelet transform can then be used to effectively handle the point singularity in the Radon domain. Their initial proposal was intended for functions defined in the continuous $\mathbb{R}^2$ space [51, 52].

The Continuous Ridgelet Transform (CRT) of a function $f(\mathbf{x})$ in $\mathbb{R}^2$ is defined as

$$CRT_f(a,b,\theta) = \int_{\mathbb{R}^2} \Psi_{a,b,\theta}(\mathbf{x}) f(\mathbf{x}) \, \mathrm{d}x \tag{1}$$

where $\mathbf{x} = (x_1, x_2)^T$ is the position vector and the ridgelets $\Psi_{a,b,\theta}(\mathbf{x})$ in 2D are defined from a 1D wavelet-type function, $\psi(x)$, as

$$\Psi_{a,b,\theta}(\mathbf{x}) = \frac{1}{\sqrt{a}} \psi\left(\frac{x_1 \cos\theta + x_2 \sin\theta - b}{a}\right) \tag{2}$$

In Eqns. (1) and (2), the parameters a, b and θ relate to scaling, shift and rotation transforms respectively. Fig. 1 shows an example ridgelet function which is oriented at an angle θ and is constant along the lines $x_1 \cos\theta + x_2 \sin\theta$ (the "ridges"). Note that the wavelets appear perpendicularly to the ridges.

In 2D, ridgelets and wavelets are linked by the Radon transform. The Radon transform of $f(\mathbf{x})$ in $\mathbb{R}^2$ space is given by

$$R_f(\theta,t) = \int_{\mathbb{R}^2} \delta(x_1 \cos\theta + x_2 \sin\theta - t) f(\mathbf{x}) \, \mathrm{d}x \tag{3}$$

where δ is the Dirac distribution which forms projection lines at an angle θ across the image at perpendicular distance t to the origin. The ridgelet transform is then equivalent to the application of a 1D wavelet transform to the projection lines of the Radon transform:

$$CRT_f\left(a,b,\theta\right) = \int_{\mathbb{R}} \psi_{a,b}\left(t\right) R_f\left(\theta,t\right) \mathrm{d}t \tag{4}$$

So the ridgelet function can be realised by applying 1D wavelet transforms to the projections in Radon space.

For image processing applications, we clearly need to apply the various transformations in discrete form. We use the construct known as the Finite RAdon Transform (FRAT) for this due to its relative ease of implementation [2]. The 2D FRAT uses sums of pixel intensities to represent the integral in Eqn. (4). The summations are over "projection lines" in the image, as implied by the above theory. Following the same approach as [2], we define the pixels on a finite grid $Z_p = \{0, 1, p-1\}$ and the transform is

$$r_k\left[l\right] = FRAT_f\left(k,l\right) = \frac{1}{\sqrt{p}} \sum_{i,j \in L_{k,l}} f\left[i,j\right] \tag{5}$$

where $L_{k,l}$ denotes the pixels that form a projection line in the image, $f\left[i,j\right]$:

$$\begin{aligned} L_{k,l} &= \{(i,j) \ : \ j = ki + l \ (\mathrm{mod}\ p)\ ,\ i \in Z_p\}\ ,\ 0 \leq k < p \\ L_{p,l} &= \{(l,j) \ : \ j \in Z_p\} \end{aligned} \tag{6}$$

To complete the ridgelet transform we need to take the discrete wavelet transform (DWT) on each FRAT projection sequence, $r_k[0], r_k[1], \ldots r_k[p-1]$. This is called the Finite RIdgelet Transform (FRIT). It is the result of this FRIT that we later use as the basis of our feature vectors, described in Section 4.

3.2. Subspace methods for data reduction

PCA and LDA are the most commonly used data reduction techniques for face recognition. Both are data-based techniques and require no prior information about the data in the image (except that LDA uses class information). Our

experiments involve various combinations of PCA and LDA to supplement the ridgefaces algorithm, so we briefly outline these two powerful methods.

3.2.1. Principle Component Analysis

Also termed the K-L transform, PCA was originally developed for dimensionality reduction and noise reduction. Turk and Pentland developed a method which captured the variance of the whole face within a given dataset rather than concentrating on specific facial features [8]. PCA aims to calculate a set of orthonormal basis dimensions of the dataset. The first dimension corresponds to the maximal variance; the second dimension corresponds to the maximal variance in an orthogonal direction to that of the first, and so on. The dataset can then be projected onto a subspace where more discriminating features lie in the lower dimensions.

Written formally, the eigenvectors of the covariance matrix, Ω, of the distribution, spanned by training a set of face images is calculated. The projection into the subspace is then expressed as an eigenvalue problem:

$$\boldsymbol{\Omega} V = \boldsymbol{\lambda} V \tag{7}$$

where $\boldsymbol{\lambda}$ is a diagonal matrix containing the eigenvalues and V contains the eigenvectors corresponding to the eigenvalues in $\boldsymbol{\lambda}$. Each image can be projected into the eigenspace with the resultant vectors acting as low dimensional person-specific feature vectors.

3.2.2. Linear Discriminant Analysis

This related technique [3] also involves projecting the image dataset into a subspace with high discriminating properties. LDA projects the images in such a way that those of same class are grouped close together in the subspace and those of different classes are separated from each other. In this respect, LDA is different to PCA in that it utilises class information to perform this task. PCA by contrast aims to maximize the overall scatter of all the images in lower dimensions and makes no attempt to distinguish images in the same class from images in other classes.

LDA calculates two matrices: the between-class scatter matrix (S_b) which captures the variation between the classes of images and the within-class scatter matrix (S_w) which captures variation in the images of same class. LDA then solves the generalized eigenvalue problem for S_b and S_w such that

$$S_b V = \boldsymbol{\lambda} S_w V \tag{8}$$

In other words, LDA aims to maximise $\det|S_b|/\det|S_w|$. As with the eigenface method discussed in Section 3.2.1, images can be projected into the new space and used as low-dimensional feature vectors.

3.3. Photometric Stereo

First introduced by Woodham in 1980 [4], PS is a reflectance map based technique in which the intensity values from multiple images are obtained from the same viewpoint under different lightning directions. This intensity information is used to determine the surface geometry of the object. Essentially, PS uses three or more images to solve the under-determined problem of shape-from-shading [53] to recover surface geometry via the surface normal map. While the ridgelet-based method we describe in this paper is applicable to any 2D or 3D database (indeed we perform extensive experiments on several existing methods in Section 5), one of our key contributions is to show that it is especially effective when combined with surface normals estimated from PS. Next, we briefly cover the basic theory of the PS surface normal acquisition procedure used in this paper.

The standard form of PS (used in this paper) assumes that Lambert's Law applies:

$$I = \rho \cos\theta_s = \rho\, \mathbf{s} \cdot \mathbf{N} = \rho \begin{bmatrix} s_x \\ s_y \\ s_z \end{bmatrix}^T \begin{bmatrix} N_x \\ N_y \\ N_z \end{bmatrix} \tag{9}$$

where ρ is the albedo, θ_s is the angle between the surface normal and the light source direction, $\mathbf{N} = [N_x\ N_y\ N_z]^T$ is the unit surface normal and $\mathbf{s} = [s_x\ s_y\ s_z]^T$ is the unit light source vector.

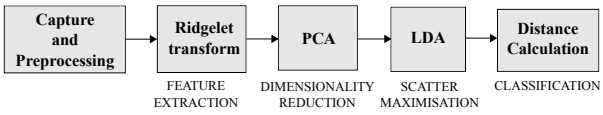

Figure 2: System architecture of the Ridgefaces algorithm for face recognition.

For this paper, we have captured a range of face images under four different light sources so we can re-write Eqn. (9) in matrix form:

$$\begin{bmatrix} I_1 \\ I_2 \\ I_3 \\ I_4 \end{bmatrix} = \rho \begin{bmatrix} \mathbf{s}_1^T \\ \mathbf{s}_2^T \\ \mathbf{s}_3^T \\ \mathbf{s}_4^T \end{bmatrix} \mathbf{N} \tag{10}$$

where $\mathbf{s}_i$ is the i^{th} light source vector and I_i is the corresponding measured pixel intensity. The albedo and surface normal components can therefore be estimated by solving this equation for each pixel [54].

4. Methodology

As explained in Section 2, ridgelets have been proven effective for 2D face recognition [13]. This paper extends the power of ridgelet transform to 3D images by using photometric stereo data. It also optimises the data acquisition, processing and parameter/storage requirements. This section describes our novel algorithm, which combines the ridgelet transform with linear subspace techniques. We call this newly proposed algorithm "Ridgefaces". The architecture of this algorithm is shown in Fig. 2.

4.1. Capture and Preprocessing

Our data was acquired using the photometric stereo capture device presented in [5]. In summary, the hardware used consists of a camera operating at 200fps, which is synchronised to four separate flash lights as shown in Fig. 3. This gives four separate images of the face, each with a known light source vector

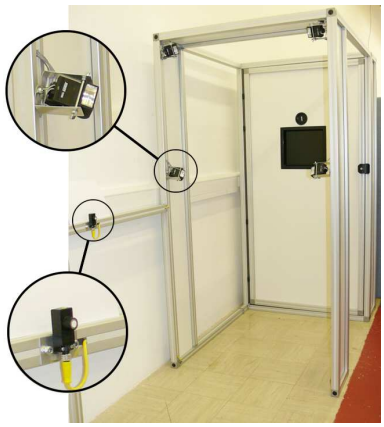

Figure 3: Photograph of the data capture device [5]. The highlighted regions show close-ups of one of the flash lights and an ultrasound trigger. The trigger detects the presence of a subject to instruct the device when to capture an image set.

which can be used to estimate the albedo and surface normals using the theory summarised in Section 3.3.

Aside from a few initial tests with older databases, we use a subset of the data captured using this device in [6]. The device was placed at the entrance to a busy workplace and employees we asked to "casually walk through the device" for their automatic scan. The database therefore contains a multitude of natural expressions and poses as would be expected in a real-world environment. This is in contrast to most previous work, which used highly controlled poses and expressions. Fig. 4 shows an example of both the raw and processed data captured by the device. Fig. 5 shows the albedo images of a few more challenging faces that were captured. It is worth noting at this point that our high recognition rates reported in Section 5 demonstrate that the method is robust to typical expressions and pose variations expected to be found in real-world applications. Furthermore, as our method is inherently three-dimensional in nature, we do not suffer from illumination changes, as in most two-dimensional approaches.

Carefully designed preprocessing can significantly improve the performance of many face recognition systems. In particular, the method by which the face part of the images are cropped from the field of view has a major impact on

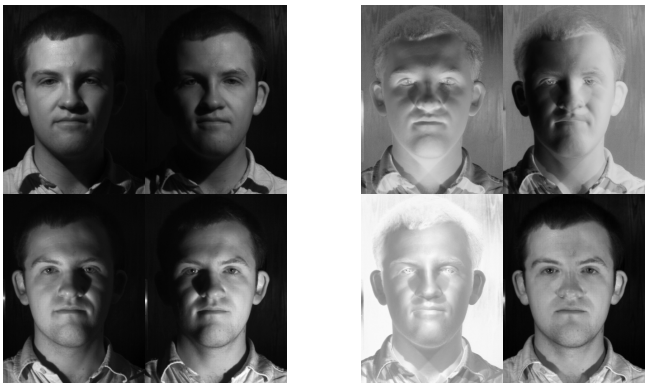

Figure 4: Left: example of four raw images captured by the PhotoFace device. Right: processed data comprising of x, y and z components of the surface normals and the albedo map.

Figure 5: Examples of typical expressions and pose variations encountered in the PhotoFace database (albedo images) [6].

recognition rates. In a similar fashion to other work in the field, we chose to manually crop the faces using a specific set of rules to include the main facial features [55]. We do this manually because it means our reported recognition rates are representative of our actual recognition algorithm, rather than being influenced by the unrelated face detection and cropping process. Down-sampling the images can also form a crucial preprocessing step as the resolution can have a significant effect on the performance of the algorithm, as we show in Section 5. Apart from cropping and (for some of our experiments) rescaling, we do no further pre-processing.

4.2. Feature extraction

Our feature extraction method essentially consists of applying the FRIT to the face images in our database to obtain a discriminating feature vector. As discussed in Section 3.1, the ridgelet transform is the application of a 1D wavelet transform on Radon space projections of the image, and can be approximated in discrete space using Eqn. (5). The result of the FRIT is reshaped into a feature vector for further analysis. The number projection angles (θ in Eqn. (1)) determines the amount of data conserved, and therefore the size of the image in discrete Radon space. The number of angles is determined by the angular interval between projections, $\theta_{interval}$. Obviously smaller values for $\theta_{interval}$ correspond to increased computation time, but also the classification accuracy is affected in a highly nonlinear fashion. The effect of varying the number of projection angles on recognition accuracy and computational efficiency is discussed in detail in Section 5.

It is worth noting here, that as points in the Radon space are based on integrals of real space over a line, the Radon transform of several noise types is constant for all displacements and directions. This constant is equal to the mean noise value along the line which is typically zero. This robustness to noise is a significant advantage of using the Radon transform.

4.3. Dimensionality reduction

While the above technique of the ridgelet transform is an effective discriminatory representation of face images (as proven in Section 5), the size of the feature vectors are still relatively large (e.g. length of image = 23,348 for typical case of $\theta_{interval} = 3°$). We therefore apply PCA to further reduce the dimensionality of our feature vectors. This allows us to discard a tunable number of components depending on specific application requirements.

Belhumeur et al. [3] suggested that the first three principal components typically capture the image variation due to lighting effects. Discarding these components therefore may reduce such detrimental effects. Indeed, we test this in Section 5 of this paper. Note however, that the key results in this paper are based on surface normal data, not intensity, and so this step should be unnecessary. This is an important advantage of our method, along with other 3D face recognition techniques.

4.4. Scatter maximisation

In order to maximise scatter between individuals (classes), we apply the technique of LDA to the selected number of principle components. This has the effect of projecting training images of identical subjects closer together in the subspace, while forcing different subjects further apart. This stage of our method is identical to the standard Fisherface technique [3].

4.5. Classification

Face recognition is carried out by projecting the FRIT of training and probe images into the PCA then LDA subspaces and computing the Euclidean distance between the resulting feature vectors and the probe image feature vector. The identity of the probe is simply taken as the closest matching feature vector in the training set. In our experiments, we also show classification results without applying all the stages of the method. For example, we compare the results of the full method to those without projecting the feature vectors into LDA space. We also compare the results to standard PCA and Fisherfaces (i.e. without applying the FRIT).

Table 1: Size of different databases and image format in each database.

Database	Size (No. of subjects × No. of samples per subject)	Image dimensions
ORL	40×10	112×92
Yale	15×13	243×320
faces94	152×20	200×180
PhotoFace	60×6	273×273

5. Results

In this section, we present experimental validation of our method and optimise the recognition procedure. Our experiments consist of (1) applying our methods to existing 2D databases, (2) applying the methods to the albedo images from our own PhotoFace database [6], and (3) application to the surface normals in the PhotoFace database. Note that we would generally expect better results using the albedo image compared to raw 2D images since the albedo map is inherent to the subject, while the raw images are illumination dependent. For the existing databases, we use ORL [56] (uniform lightning condition, different poses with no expression variations), Yale [57] (frontal images, varying lightning conditions, single pose with strong expression changes) and faces94 [58] (frontal images, uniform lightning conditions, single pose with little expression variation). Table 1 summarises the size and format of these databases. N.B. We only use the subset of the available PhotoFace data described in [6] as we select the subjects with sufficient training images only.

5.1. Experiments on 2D databases

5.1.1. Experiment 1: Variation of number of projections

Our first experiments relate to the application of the ridgelet transform on standard 2D face databases. The ridgelet-transformed data are not projected

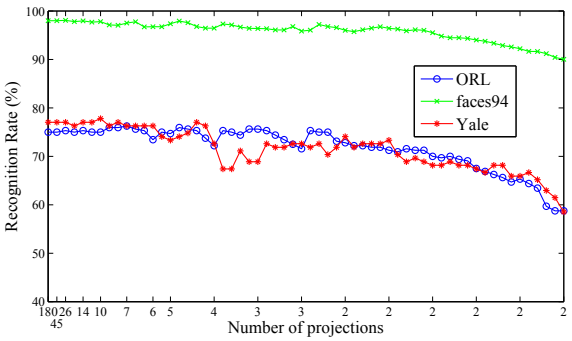

Figure 6: Recognition rates as a result of varying the number of projections. Equal number of projections marked on x-axis indicates projections taken at different angles.

into PCA subspace, but used directly for classification. The recognition results are shown in Fig. 6, which also presents the effect of the number of projections on performance. For 180, 45 and 26 projections, we get almost the same accuracy, suggesting that a low-resolution representation of the faces in Radon space is sufficient to maintain reasonable recognition. The faces94 database has the best overall results due to the inclusion of less expression, lightning and pose variation as mentioned in the descriptions above.

For the cases where only two or three projections are used (for which it is debatable whether or not "Radon space" is a suitable name), the recognition rate depends on which specific projection angles we choose. Clearly some projections are better in capturing directional features than others. A few variations of projection angles are shown in Fig. 6 to illustrate this.

5.1.2. Experiment 2: Variation of angle of projection

Motivated by the decreasing recognition rates to the right-hand-side of Fig. 6, we next present results of a simple experiment that uses only one Radon projection to obtain the feature vector. This allows us to specify which projecting angle best extracts the most discriminating information. The graph shown in Fig. 7 shows that the maximum accuracy occurs at a projection angle of 90°

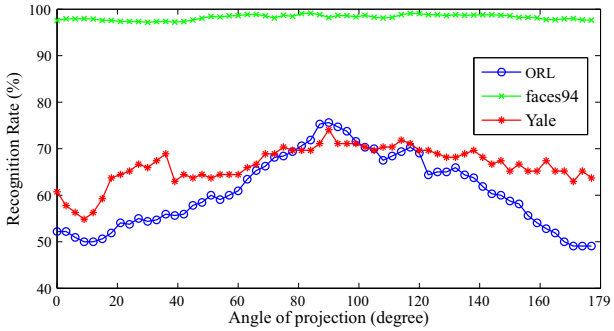

Figure 7: Recognition rates as a result of varying a single projection angle.

(horizontal). As the ridgelet transform specifically extracts the directional features of the face images, this result suggests that directional features of faces along horizontal lines such as eye brows, lips and eyes offer useful information to effectively distinguish faces. This result is conducive to the findings of Dakin and Watt [59] who show through psychological experiments that human observers rely more on horizontal features that other directions. In addition, it may be that pose variation (the most common in practice is yaw) is cancelled out best with such horizontal integrations (sums). Confirmation and expansion of this point remains the focus of future work. Finally of note for Fig. 7 is that a surprisingly high recognition rate is possible from just a single projection.

5.2. Experiments on the PhotoFace database – albedo images

The PhotoFace database [6] consists of grayscale albedo images as well as a dataset of surface normals, $[p_x, p_y, p_z]^T$. Various experiments are performed using the dataset and different algorithm combinations are compared to each other (by comparing the effects of omitting various blocks from Fig. 2).

5.2.1. Experiment 3: Preliminary tests

To commence, we tested standard PCA and Fisherfaces on the PhotoFace database to set a benchmark for Ridgefaces algorithm. The results are presented in Table 2. The table also shows the first result of the ridgefaces algorithm using

Table 2: Result of testing standard algorithms and ridgefaces on the PhotoFace database.

Algorithm	Recognition Rate
PCA	63%
Fisherfaces	78%
Ridgefaces	90%

60 Radon projections and 300 principle components. The ridgefaces algorithm vastly outperforms the classical methods here.

5.2.2. Experiment 4: Effect of discarding principle components

As mentioned in Section 4.3, discarding several first principle components (PCs) can significantly reduce effects due to lightning variation in some circumstances. However, one would expect this to have little effect on our data since the albedos and surface normals should be illumination invariant (one of the strengths of our method). To verify this, we have plotted the recognition rates resulting from the various algorithms, with several PCs discarded, in Fig. 8. The results are as expected, with the exception of a significant increase in recognition for the ridgefaces algorithm when the first PC is discarded. The precise reason for this is not clear at present. Figs. 9 and 10 shows the result of discarding PCs *and* using fewer projections.

5.2.3. Experiment 5: Effect of scaling images

This section demonstrates the effect of image resolution on the algorithms. Fig. 11 shows this effect by plotting the recognition rate for each method after the albedo images have undergone a linear subsampling. In order to make the comparisons fair, we use the number of projections and discarded PCs that gave best overall results for each algorithm. The number of projections for Ridgelet-PCA is 15 and for ridgefaces is 30. The number of principle components discarded are 1 for PCA, 3 for Fisherfaces, 5 for Ridgelet-PCA and 1 for Ridgefaces.

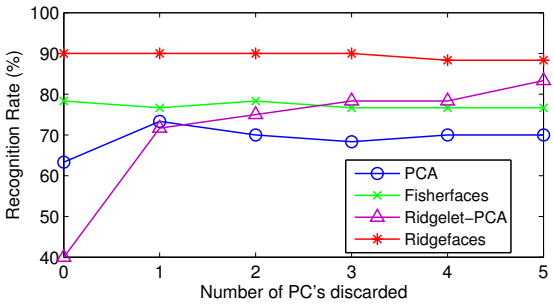

Figure 8: Result of discarding PCs on recognition rate using different algorithms (ridgelet-PCA refers to the ridgeface algorithm with the omission of LDA projection). N.B. number of projections = 60, full resolution images, total number of PCs = 300.

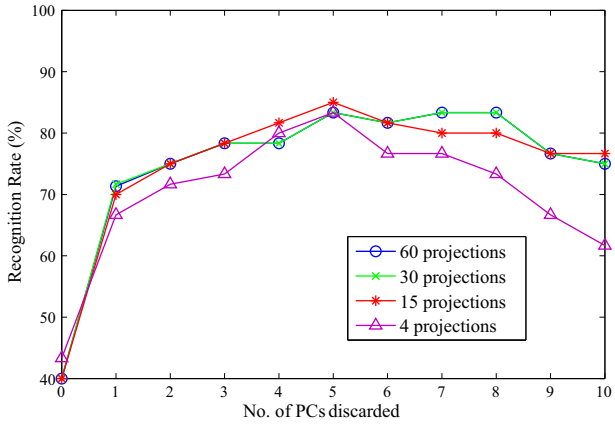

Figure 9: Result of discarding PCs on recognition rate (Ridgelet-PCA).

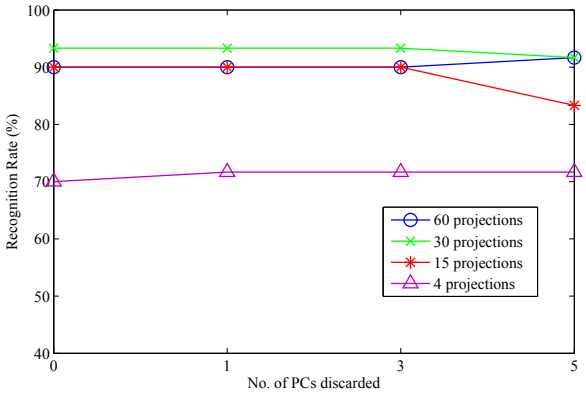

Figure 10: Result of discarding PCs on recognition rate (Ridgefaces).

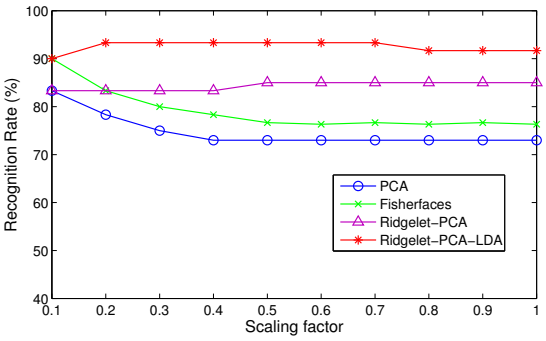

Figure 11: Comparison of algorithms for best recognition rate versus scale factor.

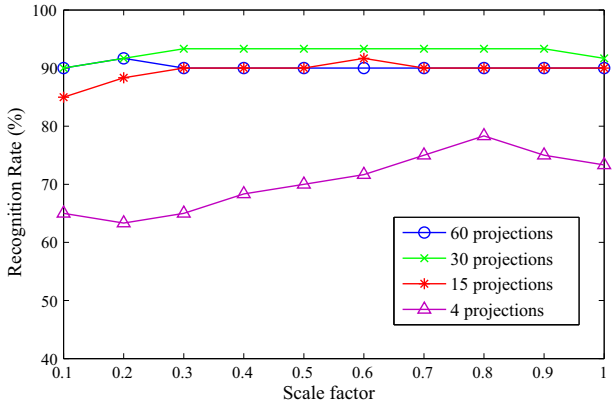

Figure 12: Result of varying number of projections on recognition accuracy (Ridgefaces).

From the plots, it can be observed that the Ridgefaces algorithm gives the consistently best recognition accuracy. It can also be seen that for PCA and Fisherfaces, the recognition accuracy increases as the images are scaled down. However, the Ridgefaces and ridgelet-PCA algorithms show little of this effect. This effect may be due to PCA and Fisherfaces benefiting from the high-frequency suppressing effects of the downsampling, while the other two methods have already filtered out the high-frequencies during the ridgelet transform procedure.

5.2.4. Experiment 6: Effect of varying the number of projections

The number of projections has a significant effect on the performance of the algorithms. The effect of varying the number of projections on recognition accuracy for the Ridgefaces algorithm is shown in Fig. 12 at various resolutions. Not surprisingly, a larger number of projections results in higher recognition accuracy. At the same time however, a very high recognition rate is possible using a relatively small number of projection angles. This result is conducive to the results in Fig. 6.

5.2.5. Experiment 7: Computation time

In this experiment, the computation time of the various algorithms are compared. For this test, the number of PCs discarded, the scaling factors and

Table 3: Time taken to recognize a single albedo probe image for different algorithms (using optimum parameters).

Algorithm	Time	Recognition Rate
Fisherfaces	19.34 ms	90%
PCA	27.36 ms	83%
Ridgefaces	27.93 ms	93%
Ridgelet-PCA	34.25 ms	85%

the number of projections are set to give the best recognition rate for each algorithm as before. The computation time to recognise a single probe image is measured for different algorithms. The corresponding recognition accuracy is also calculated and both are shown in Table 3. The Fisherfaces algorithm shows the best speed performance for this test, followed by PCA, Ridgefaces and ridgelet-PCA. Note however, that all four computation times are competitive and that the Ridgefaces algorithm gives best recognition rate. The purpose of this experiment was to give a relative time, rather than absolute. For reference however, these tests were carried out on a Windows 7 PC with dual core 1.67 GHz processor under MATLAB v7.10.

5.3. Experiments on the PhotoFace database – surface normals

Surface normals provide orientation information of the surface at each pixel location. This experiment is carried out to examine the contribution of orientation information to the face recognition accuracy and performance. We experiment on each of the x, y and z components of surface normals (p_x, p_y and p_z respectively) as well as their ℓ_n-norms. Recognition rates for individual components are shown in Fig. 13 and Table 4. Referring to these results, we note that the surface normals yield better results compared to the albedo data. Note that the most suitable combination of surface normal components to use was the ℓ_1-norm of $[p_x, p_y]^T$ or p_y alone. Indeed, the best case was able to attain 100% recognition. Note also that the superior performance using p_y compared

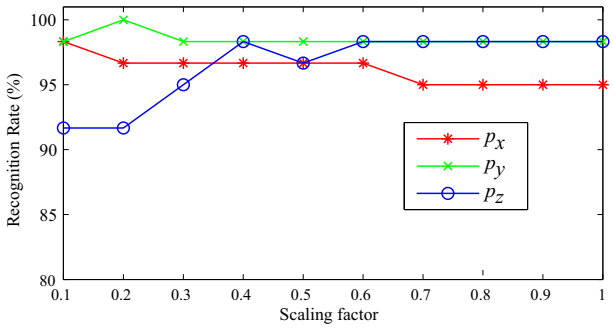

Figure 13: Plot of recognition rate vs. scale factor for individual components of surface normals.

Table 4: Recognition rates for different combinations of p_x, p_y and p_z

	Recognition rate			
	(p_x, p_y)	(p_y, p_z)	(p_x, p_z)	(p_x, p_y, p_z)
ℓ_1-norm	100%	98.67%	95.33%	98.33%
ℓ_2-norm	93.33%	90%	80%	–
ℓ_∞-norm	98.33%	93.33%	96.67%	96.67%

to p_x is conducive to the results in Section 5.1.2.

6. Discussion

The controlling parameters for the ridgelet algorithm are the number of projections and angle of projections (the latter is only significant if there are just few projections used). We adjusted these parameters to test how they affect the recognition accuracy and computation time. The results showed that even with a relatively small number of projections, the system can be very accurate to give high recognition rate. Indeed, the recognition rate was almost identical for the cases where 180, 60 and 30 projections were used. The number of projections is directly proportional to the size of the transformed image in Radon space and it has direct consequences on the system performance. For the faces94 database,

we attained a very high recognition rate (97%), even with a single projection of the ridgelet transform. A single projection therefore has a great deal of information content to correctly recognise a face. This is an important aspect of the ridgelet transform for face representation which has been largely ignored until now. We also attained different recognition rates using the same number of projections but at different angles. However, we are not yet certain about the causes of this behaviour and so we reserve further discussion for future research.

The experiments on varying the number of discarded PCs for albedo images confirmed little variation as expected. The performance of PCA and ridgelet-PCA however, did show significant improvement when the first PC was discarded. On the other hand, Fisherfaces and Ridgefaces algorithms showed little effect of this variation. Scaling the image was another crucial parameter in the tests, showing major effect on the recognition accuracy for the classical methods of PCA and LDA. For these cases, lower resolution images yielded significantly better recognition accuracy than higher resolution images. This is perhaps due to poor image alignment having a greater effect on high-frequency features. However, when the ridgelet transform was used, this effect did not manifest. Our final experiments showed that surface normals recovered from PS provide convincingly better recognition rate than any other form of data we considered. The computation times were competitive to state-of-the-art for all methods, although the ridgelet methods were slightly slower than standard Fisherfaces. Finally, we showed that our method is highly robust to low resolution images and fewer projections. This permits flexibility in our algorithm, providing a useful trade-off between accuracy and efficiency.

From all the results and the overall discussion, we defined the best system parameters as shown in Table 5. We have compared this to another state-of-the-art method that has shown great promise for our type of data: that of Elastic Graph Matching (EGM) [60]. Specifically, we have applied the Elastic Bunch Graph Map [61] where the face is represented as a graph and the nodes are feature vectors generated via Gabor filters or, as in our case, morphological features [62]. This alternative approach was also able to attain 100% accuracy.

Table 5: Optimum system parameters.

Parameters	Value
Algorithm	Ridgefaces
Modality	p_x and p_y (ℓ_1-norm)
Recognition accuracy	100%
Scale factor	0.1
Number of projections	30
Number of PCs discarded	0

Indeed, the EGM approach has the advantage that image registration is built into the algorithm, diminishing the need for image cropping. However, this advantage comes at the expense of processing time: the EGM method requires sequential face matching, taking approximately 1.5 seconds per comparison (or 90 seconds to compare to our gallery of 60 faces).

7. Conclusion

This work has made several major contributions to existing technologies for automated face recognition. The paper has proposed a novel technique that combines the classical method of Fisherfaces, the modern concept of ridgelet transforms and the 2.5D shape estimation technique of photometric stereo. Detailed experiments have been conducted to test the algorithm under different critical conditions. The results showed the superiority of the algorithm over the standards methods. We considered the ridgelet transform, PCA and LDA as separate blocks and integrated them into one complete system. Each block has its own advantages which contribute to the overall performance: the ridgelet transform is able to represent the face image data in such a way as to maximise its discriminating features; PCA allows large-scale dimensionality reduction; LDA maximises the feature vector difference between subjects; and photometric stereo renders the data illumination invariant and provides a richer dataset

than greyscale images alone. In future work, we hope to study the fusion of albedo and surface normals in more detail and consider the effects of pose and how integrating the surface normals may help to correct for its detrimental effects.

In summary, our Ridgefaces algorithm, combined with the PS "PhotoFace" capture device, offers a competitive face recognition technology. The system works at low dimensionality, is computationally efficient, is deployable in the real world and provides high recognition rate. Furthermore, since we are using 3D data, there is potential for pose correction in future work. The primary weakness of the method is the need for highly controlled illumination to facilitate the PS process.

Acknowledgements

The authors would like to thank Rahulkumar Koche, Tushar Keskar, Aniket Pande and Milind Rane for their valuable contribution towards the initial development of this research. We also thank the UK Engineering and Physical Sciences Research Council for funding the project that made this work possible.

References

[1] A. J. O'Toole, P. J. Phillips, F. Jiang, J. Ayyad, N. Pénard, H. Abdi, Face recognition algorithms surpass humans matching faces over changes in illumination, IEEE Trans. Pattern Anal. Mach. Intell. 29 (9) (2007) 1642–1646.

[2] M. N. Do, M. Vetterli, The Finite Ridgelet Transform for Image Representation, IEEE Trans. Image Processing 12 (2003) 16–28.

[3] P. N. Belhumeur, J. P. Hespanha, D. J. Kriegman, Eigenfaces vs. fisherfaces: Recognition using class specific linear projection, IEEE Trans. Pattern Anal. Mach. Intell. 19 (7) (1997) 711–720.

[4] R. J. Woodham, Photometric method for determining surface orientation from multiple images, Optical Engineering 19 (1) (1980) 139–44.

[5] M. F. Hansen, G. A. Atkinson, L. N. Smith, M. L. Smith, 3D face reconstructions from photometric stereo using near infrared and visible light, Comput. Vis. Image Underst. 114 (8) (2010) 942–951.

[6] S. Zafeiriou, M. F. Hansen, G. A. Atkinson, V. Argyriou, M. Petrou, M. L. Smith, L. N. Smith, The PhotoFace Database, in: Proc. Biometrics Workshop of Computer Vision and Pattern Recognition., 2011, pp. 161–168.

[7] W. W. Bledsoe, Man-machine facial recognition, Technical Report PRI 22, Panoramic Research, Inc., Palo Alto, California (August 1966).

[8] M. A. Turk, A. P. Pentland, Eigenfaces for Recognition, J. Cognitive Neuroscience 3 (1) (1991) 71–86.

[9] M. Kirby, L. Sirovich, Application of Karhunen–Loeve procedure for the characterization of human faces, IEEE Trans. Pattern Anal. Mach. Intell. 12 (1) (1990) 103–108.

[10] R. A. Fisher, The use of multiple measures in taxonomic problems, Annals of Eugenics 7 (1936) 170–188.

[11] A. M. Martínez, A. C. Kak, PCA versus LDA, IEEE Trans. Pattern Anal. Mach. Intell. 23 (2) (2001) 228–233.

[12] M. Sharkas, M. A. Elenien, Eigenfaces vs. Fisherfaces vs. ICA for Face Recognition: A Comparative Study, in: Proc. IEEE Int. Conf. Signal Processing, 2008, pp. 914–919.

[13] D. V. Jadhav, R. S. Holambe, Feature extraction using Radon and Wavelet transforms with application to face recognition, J. Neurocomputing 72 (2008) 1951–1959.

[14] X. J. Jun, N. Lin, Y. Miao, A New Digital Implementation of Ridgelet Transform for Images of Dyadic Length, in: Proc. IEEE Int. Conf. Information Technology and Applications, 2005, pp. 613 –616.

[15] K. W. Bowyer, K. Chang, P. Flynn, A survey of approaches and challenges in 3D and multi-modal 3D + 2D face recognition, Comput. Vis. Image Underst. 101 (1) (2006) 1–15.

[16] B. K. P. Horn, Shape from shading: A method for obtaining the shape of a smooth opaque object from one view, Ph.D. thesis, Massachusetts Institute of Technology (1970).

[17] K. Ikeuchi, B. Horn, Numerical shape from shading and occluding boundaries, Artificial Intelligence 17 (1981) 141–184.

[18] A. P. Witkin, Recovering surface shape and orientation from texture, Artificial Intelligence 17 (1-3) (1981) 17–45.

[19] E. Coleman, Jr., R. Jain, Obtaining 3-dimensional shape of textured and specular surfaces using four-source photometry, Computer Graphics Image Processing 18 (1982) 309–328.

[20] A. S. Georghiades, P. N. Belhumeur, D. J. Kriegman, From few to many: illumination cone models for face recognition under variable lighting and pose, IEEE Trans. Pattern Anal. Mach. Intell. 23 (2001) 643–660.

[21] A. S. Georghiades, Incorporating the torrance-sparrow model of reflectance in uncalibrated photometric stereo, in: Proc. IEEE Int. Conf. Computer Vision, 2003, pp. 816–825.

[22] S. Zhou, R. Chellappa, D. Jacobs, Characterization of human faces under illumination variations using rank, integrability and symmetry constraints, in: Proc. European Conf. Computer Vision, 2004, pp. 588–601.

[23] S. Barsky, M. Petrou, The 4-source photometric stereo technique for three-dimensional surfaces in the presence of highlights and shadows, IEEE Trans. Pattern Anal. Mach. Intell. 25 (2003) 1239–1252.

[24] J. Sun, M. L. Smith, L. N. Smith, S. Midha, J. Bamber, Object surface recovery using a multi-light photometric stereo technique for non-Lambertian surfaces subject to shadows and specularities, Im. Vis. Comp. 25 (2007) 1050–1057.

[25] S. Zhou, G. Aggarwal, R. Chellappa, D. Jacobs, Appearance characterization of linear lambertian objects, generalized photometric stereo, and illumination-invariant face recognition, IEEE Trans. Pattern Anal. Mach. Intell. 29 (2007) 230–245.

[26] M. Chandraker, J. Bai, R. Ramamoorthi, A theory of differential photometric stereo for unknown isotropic BRDFs, in: Proc. Computer Vision and Pattern Recognition, 2011, pp. 2505–2512.

[27] V. Blanz, T. Vetter, A morphable model for the synthesis of 3d faces, in: Proc. SIGGRAPH, 1999, pp. 87–194.

[28] W. A. P. Smith, E. R. Hancock, Recovering facial shape using a statistical model of surface normal direction, IEEE Trans. Pattern Anal. Mach. Intell. 28 (12) (2006) 1914–1930.

[29] M. Reiter, R. Donner, G. Langs, H. Bischof, 3D and Infrared Face Reconstruction from RGB data using Canonical Correlation Analysis, in: Proc. IEEE Int. Conf. Pattern Recognition, 2006, pp. 425–428.

[30] J. Kim, S. Yu, J. Hwang, S. Kim, S. Lee, Nonintrusive 3-D face data acquisition system, in: Proc. IEEE Conf. Industrial Electronics and Applications, 2009, pp. 642–646.

[31] M. Mayo, E. Zhang, 3D face recognition using multiview keypoint matching, in: Proc. IEEE Int. Conf. Advanced Video and Signal Based Surveillance, 2009, pp. 290–295.

[32] C. Xu, Y. Wang, T. Tan, L. Quan, Automatic 3D face recognition combining global geometric features with local shape variation information, in:

Proc. IEEE Int. Conf. Automatic Face and Gesture Recognition, 2004, pp. 308–313.

[33] A. F. Abate, M. Nappi, S. Ricciardi, G. Sabatino, Fast 3D face recognition based on normal map, in: Proc. IEEE Int. Conf. Image Processing, Vol. 2, 2005, pp. 946–949.

[34] X. Lu, A. K. Jain, D. Colbry, Matching 2.5D face scans to 3D models, IEEE Trans. Pattern Anal. Mach. Intell. 28 (1) (2006) 31–43.

[35] P. J. Besl, N. D. McKay, A method for registration of 3D shapes, IEEE Trans. Pattern Anal. Mach. Intell. 14 (1992) 239–256.

[36] T. Papatheodorou, D. Rueckert, Evaluation of automatic 4D face recognition using surface and texture registration, in: Proc. IEEE Int. Conf. Automatic Face and Gesture Recognition, 2004, pp. 321–326.

[37] M. Hüsken, M. Brauckmann, S. Gehlen, C. Von der Malsburg, Strategies and benefits of fusion of 2D and 3D face recognition, in: Computer Vision and Pattern Recognition, 2005, p. 174.

[38] F. Xue, X. Ding, 3D+2D face localization using boosting in multi-modal feature space, in: Int. Conf. Pattern Recognition, Vol. 3, 2006, pp. 499–502.

[39] C. BenAbdelkader, P. A. Griffin, Comparing and combining depth and texture cues for face recognition, Im. Vis. Comput. 23 (3) (2005) 339–352.

[40] G. P. Kusuma, C.-S. Chua, PCA-based image recombination for multimodal 2D+3D face recognition, Im. Vis. Comput. 29 (5) (2011) 306–316.

[41] Y. Wang, C.-S. Chua, Face recognition from 2D and 3D images using 3D Gabor filters, Im. Vis. Comput. 23 (11) (2005) 1018–1028.

[42] Y. Wang, C.-S. Chua, Robust face recognition from 2D and 3D images using structural Hausdorff distance, Im. Vis. Comput. 24 (2) (2006) 176–185.

[43] C. Xu, S. Li, T. Tan, L. Quan, Automatic 3D face recognition from depth and intensity Gabor features, Pattern Recognition 42 (9) (2009) 1895–1905.

[44] S. Malassiotis, M. G. Strintzis, Robust face recognition using 2D and 3D data: Pose and illumination compensation, Pattern Recognition 38 (12) (2005) 2537–2548.

[45] F. Tsalakanidou, S. Malassiotis, Real-time 2D+3D facial action and expression recognition, Pattern Recognition 43 (5) (2010) 1763–1775.

[46] L. Nanni, A. Lumini, RegionBoost learning for 2D+3D based face recognition, Pattern Recognition Letters 28 (15) (2007) 2063–2070.

[47] B. Gökberk, H. Dutağaci, A. Ulaş, L. Akarun, B. Sankur, Representation Plurality and Fusion for 3-D Face Recognition, IEEE Trans. Systems, Man, and Cybernetics 38 (1) (2008) 155–173.

[48] A. F. Abate, M. Nappi, D. Riccio, G. Sabatino, 2D and 3D face recognition: A survey, Pattern Recognition Letters 28 (14) (2007) 1885–1906.

[49] D. Smeets, P. Claes, D. Vandermeulen, J. G. Clement, Objective 3D face recognition: Evolution, approaches and challenges, Forensic Science International 201 (1–3) (2010) 125–132.

[50] E. J. Candies, Ridgelets: Theory and Applications, Ph.D. thesis, Department of Statistics, Stanford University (1998).

[51] S. R. Deans, The Radon Transform and some of its applications, John Wiley and Sons, 1983.

[52] J. L. Starck, E. J. Candies, D. Donoho, The Curvelet transform for image denoising, IEEE Trans. Image Processing 11 (2002) 670–684.

[53] R. Zhang, P. S. Tsai, J. E. Cryer, M. Shah, Shape from shading: A survey, IEEE Trans. Patt. Anal. Mach. Intell. 21 (1999) 690–706.

[54] V. Argyriou, M. Petrou, Photometric stereo: An overview, Advances in Imaging and Electron Physics 156 (2009) 1–54.

[55] M. F. Hansen, G. A. Atkinson, Biologically inspired 3D face recognition from surface normals, in: Proc. Intl. Conf. Exhibition Biometrics Technology, 2010, pp. 26–34.

[56] AT & T Laboratories Cambridge, `http://www.cl.cam.ac.uk/research/dtg/attarchive/facedatabase.html` (Accessed: 10 November 2011).

[57] University of California San Diego, `http://vision.ucsd.edu/~leekc/ExtYaleDatabase/ExtYaleB.html` (Accessed: 10 November 2011).

[58] University of Essex, `http://cswww.essex.ac.uk/mv/allfaces/faces94.html` (Accessed: 10 November 2011).

[59] S. C. Dakin, R. J. Watt, Biological "bar codes" in human faces, J. Vision 9 (2009) 1–10.

[60] P. J. Phillips, H. Moon, S. A. Rizvi, P. J. Rauss, The FERET evaluation methodology for face recognition algorithms, IEEE Trans. Pattern Anal. Mach. Intell. 22 (2000) 1090–1104.

[61] L. Wiskott, J. M. Fellous, N. Krüger, C. von der Malsburg, Face recognition by elastic bunch graph matching, IEEE Trans. Pattern Anal. Mach. Intell. 19 (1997) 775–779.

[62] S. Zaferiou, A. Tefas, I. Pitas, The discriminant elastic graph matching algorithm applied to frontal face verication, Pattern Recognition 40 (2007) 2798–2810.

*Author Biography

Satyaji Kautkar

Satyajit Kautkar has a Bachelor of Engineering degree from VIT, University of Pune, India and a Master of Science in Advanced Technologies in Electronics from the University of the West of England, Bristol, UK. He has worked on several other projects including creating a power quality benchmark and an SMS-based voting sytem. Satyajit won the best paper in session award at the International Conference and Exhibition on Biometrics Technology 2010 and the autonomous line tracer robot competition at national level “VITality” in Pune.

Gary A. Atkinson

Gary Atkinson completed an MSci degree in physics at the University of Nottingham in 2003. Upon graduation, he moved to the University of York to study for a PhD degree in the Department of Computer Science, under the supervision of Edwin Hancock. His research was concerned with improving shape recovery algorithms and reflectance function estimation for computer vision. Most of his work involved the exploitation of the polarising properties of reflection from surfaces.

Gary has been working at the UWE Machine Vision Laboratory on face reconstruction and recognition research in collaboration with Imperial College since June 2007 and has been supervising Mark Hansen's PhD studies since November 2008. He works in close collaboration with Imperial College London on face recognition and also has ties with the University of Bath, the University of York and the University of Central Lancashire and several industrial partners. In addition to his computer vision research, for which he has published seven major international journal papers, Gary has worked in the medical field to develop new means of assessing head deformations of babies affected by plagiocephaly. He hopes to initiate a major new study in this area in the near future.

In 2010, Gary acted as the UK and Europe co-convener for the International Conference and Exhibition on Biometrics Technology.

Melvyn L. Smith

Melvyn L. Smith is a Professor of Machine Vision at the Bristol Institute of Technology and Director of the Centre for Intelligent Manufacturing and Machine Vision Systems (CIMMS) at UWE. He received his BEng(Hons) degree in Mechanical Engineering from the University of Bath in 1987, MSc in Robotics and Advanced Manufacturing Systems from the Cranfield Institute of Technology in 1988 and PhD from the UWE in 1997. He acts as associate editor for four leading international journals, including Image and Vision Computing and Computers in Industry , and is a program committee member for two international conferences. He has published a book together with numerous book chapters, patents, and journal / conference papers in connection with his work. He regularly presents his work through invited seminars, as well as articles and interviews to the popular media. He has been a member of the EPSRC Peer Review College since 2003, served as European commission candidate evaluator for the Sixth Framework and is currently a programme and evaluator / review expert and monitoring expert for EU Framework 7 Programme. Prof. Smith is a Chartered Engineer and an active member of the IET.